THE EFFECT OF INLET PRESSURE ON STEAM FLOW BEHAVIOR ACROSS A CONVERGENT-DIVERGENT NOZZLE

Prof.Dr. Arkan Kh. Al-Taie arkanaltaie@yahoo.com
Dr. Hussein W. Mashi Hussienmashi@yahoo.com
Mohammed M. Al-Kafagy Eng.mms71@yahoo.com

Received 22 March 2015 Accepted 18 May 2015

ABSTRACT

Convergent-Divergent nozzle has many applications especially in steam turbine. The aim of this work is to see the effect of varying inlet pressure on steam behavior through the C-D nozzle. This was done experimentally and numerically. In the experimental part, a C-D nozzle was designed and fabricated in a test section. Steam was fed from boiler at range of (0.69-0.36) bar at saturation temperature for each pressure. Shadowgraph optical method was used to see the formation of shock waves and condensation zone. In the numerical part, the nozzle was simulated using FLUENT under ANSYS code 15.0. In the experimental results, it was found that the most important influence of rapid condensation on the pressure distribution is occurred downstream the through area, when the flow in the divergent part is termed supersonic the heat release causes a pressure rise in the zone of rapid condensation. Shock wave appears in the divergent part due to over-expansion. Each of condensation zone and shock wave were showed by using shadowgraph optical method. In the numerical approach, droplet growth rate contour are presented. The maximum droplet growth rate is (1020 micron /sec) and occurred downstream the throat area. The comparison of experimental and numerical results show good agreement.

Key words: C-D nozzle, steam condensation, shock wave, over-expansion, shadowgraph.

تأثير الضغط الداخل على سلوك جريان البخار عبر فوهة متقاربة-متباعدة

أ. د. أركان خلخال حسين الطائي **د. حسين وهيب ماشي** **محمد مهدي صالح**

الخلاصة

الفوهة المتقاربة المتباعدة توجد في الكثير من التطبيقات خصوصا في التوربينات البخارية. الهدف من هذا العمل هو ان نرى تأثير تغيير الضغط الداخل على سلوك البخار خلال فوهة متقاربة-متباعدة. وقد تم ذلك عمليا ونظريا. في الجزء العملي، تم تصميم فوهة متقاربة-متباعدة ووضعت في قسم الاختبار. البخار يجهز من المرجل وبمعدل من (0.69-0.36) بار وبدرجة حرارة التشبع لكل ضغط. تم استخدام التقنية البصرية (Shadowgraph) لرؤية تشكيل موجات الصدمة ومنطقة التكثيف. في الجزء العددي، تمت محاكاة الفوهة باستخدام فونت انسز. في النتائج العملية، تبين أن أهم تأثير التكثيف السريع على توزيع الضغط في منطقة ما بعد الخنق ، عندما يتم يكون الجريان في الجزء المتباعد أسرع من الصوت يحدث فقدان للحرارة يسبب ارتفاع الضغط في منطقة التكثيف السريع . تظهر

موجة صدمة في الجزء المتباعد بسبب الإفراط في انخفاض الضغط. وقد أظهرت كل من منطقة التكثيف وموجة صدمة باستخدام أسلوب بصري صورة شعاعية. في الجزء العددي، يتم عرض توزيع معدل نمو القطرات. الحد الاقصى لمعدل نمو القطرة هو (1020 ميكرون / ثانية) وحدثت عند منطقة الخنق. المقارنة بين النتائج العملية والعددية تظهر توافق جيد.

NOMENCLATURE:

B The second Virial coefficient (m3/kg)
C The third Virial coefficient (m6/kg2)
E Total specific internal energy (J/kg)
h Static enthalpy (J/kg)
I Nucleation rate (1/m3 s)
K_b Boltzmann constant (=1.3807×10−23 J/K)
m Mass (kg)
P Pressure (Pa)
R Radius of droplets (m)
$\bar{r}$ Mean droplet radius of droplets (m)
r^* Droplet critical radius (m)
S Super saturation ratio
T Temperature (K)
u X-axial velocity (m/s)
v Y-axial velocity (m/s)

Greek symbols

β Mass fraction of the condensed phase
γ The ratio of specific heat capacities
Γ Mass generation rate (kg/m3 s)
η Number density for droplets (1/m3)
θ Non-isothermal correction factor
ρ Density (kg/m3)
σ Liquid surface tension (N/m)

Subscripts

0 Stagnation state condition
g Gas (vapor)
l Liquid
s Saturated state condition

Superscripts

$\overrightarrow{()}$ Vector
$\overline{()}$ Average of a variable

1. INTRODUCTION :

From the viewpoints of reducing power generation costs and saving energy resources ,improving efficiency of thermal power plants is an important issue. In steam turbines , which are the main units of the plant equipment, changes between gas-liquid phases play critical role. For example, the energy loss caused by condensation is approximately one-fourth of the total loss in low- pressure turbines of a nuclear power plant. Therefore, in order to design high performance steam turbines, it is essential to take into account the influences of changes between gas-liquid phases and thermodynamic properties of two-phase fluid [1].

Often the expansion process and condensation phenomenon in the LP turbines can be simulated under the transonic Laval nozzle. According Fig.1, it has seen steam expansion from superheated to wet conditions in such nozzle. Nucleation onset will be happen when the subcooled vapor reaches to Wilson point and thereupon effects to the supersonic flow in the nozzles. The Wilson point is defined as the point of maximal subcooling along a streamline as well as the point where dry and condensing static pressure curves first separate.

The classical theory calculates the condensation and evaporation rates using the Gibbs free energy and the principle of detailed balance, and the nucleation rate is then calculated assuming a steady state condition. Principles of the classical nucleation theory, mid the conventional compressible Navier-Stokes gas dynamic equations were used by a number of researchers to numerically predict multidimensional condensing flows. In addition a theory for nucleation of droplets out of its vapor is required; this is obtained through refinements to Classical nucleation theory [2].

Some of the theoretical research **(McCallum and Hunt (1997)[14]; Kermani et .al (2003)[13]; White (2000)[2]),** assumed one dimensional flow conditions in the analysis. Later studies examined two-dimensional flow in turbine cascades and nozzles. Also, a number of numerical studies were directed toward modeling two phase flow behavior of nucleating steam. Such research is divided into two parts: the first relies on the Eulerian method in analysis (**Mccallum and Hunt (1997)[14]),** while the second depends on the Eulerian-Lagrangian method in analysis of flow **(Guha and Young (1991)[7]; White and Young (1993)[3]; Gerber (2002)[1]; Kermani and Gerber (2003)[12]; Halma and Fort (2014)[9]).** Such research used Euler solver for conservation equations for the mixture while nucleation and droplet growth calculations were performed in a Lagrangian framework by tracking particle path lines. The experimental research including only experimental research **(Cinar and Yilbas (1998)[6])** was compared with the existing data in the literature. Another experimental research was with numerical model and the comparison between the theoretical and experimental results obtained from this research.

The present study includes a numerical and an experimental investigations. In the experimental part, a suitable nozzle will be designed and fabricated. A suitable test section to incorporate the nozzle will be purpose made. A shadowgraph method will be utilized to study shock appearance. While, in the theoretical part, flow simulation will be excused using ANSYS FLUENT to study the flow and shock appearance. Comparison will then be made between the experimental and theoretical results and with literature as well.

2. EXPERIMENTAL FACILITIES:

The schematic diagram of the general arrangement and main components of the system are shown in Fig. (2). Steam was supplied to the test section from boiler via, throttling valve and flow regulation valve. Maximum steam pressure from boiler is (10 bars) and maximum steam flow rate is (1000 kg/h) and at saturation temperature of each pressure.

The steam conditions at inlet to the test section can be varying by using throttling valve and the pressure supplied to the test section at the saturation temperature. The flow leaving the test section is passing to a condenser. By varying the cooling water flow rate in vacuum pump, the test section pressure ratio and hence the back pressure can be controlled.

The C-D nozzle profile selected from the experimental tests conducted in **Moscow P.E.I (University of Technology)[8] ,** but with some modifications contained in the present work. The symmetric nozzle

was rectangular in cross sectional area with constant width (60 mm) built in the center of a tunnel have a dimension (100*60*1000) mm see Fig.(3). The sides of the tunnel must be transparent in order to allow the passage of the laser beams through the test section and received it from the other side and then verified shadowgraph system conditions, so the side of the tunnel will be such as frame contain glass. The profile of the nozzle consists of two identical parts upper and lower. Nozzle profile has been drawn using Solid Work program and dimensions are shown in the table (1). The length of the nozzle is (140 mm).The nozzle throat, located (88 mm) from the nozzle entrance with throat area of (27*60) mm see Fig.(4). Material used in manufacturing nozzle is a block of Aluminum has a square cross-section area with dimensions (10 cm * 10 cm). To obtain high precision of surface nozzle profile, nozzle was manufactured using CNC machine (***C-tek***). Surface finish of the nozzle's inner side is highly smoothed finish.

In the present work, throat area of the nozzle was modified by changing the height of it. The modified height was changed from (27 mm) to (11 mm) while the width was kept the same. The modification was done by adding iron plates between the flat surface of nozzle parts (upper and lower) and the wall of the tunnel with thickness. Two plates of thickness (8 mm) were used. To assemble the test section and the nozzle, the walls have been drilled and screwed with the nozzle.

To carry out the surface pressure measurements, tapping was drilled into the lower part surface; also the wall tapping were drilled along the middle passage line starting from upstream to downstream of the nozzle and the space between tapping is (8 mm). See Fig.(5)

The shadowgraph technique was used for observing flow field; it is particularly useful where there are large density gradients, such as in steam flow across a shock wave. The schematic diagram of equipment used in this technique is shown in Fig. (6).

3. MATHEMATICAL MODELING:

3.1. Governing conservation equations for mass, momentum and energy:

In the present paper, the mathematical model describing the condensing steam consists of the continuous vapor phase at temperature T and pressure P, interspersed with a large number of spherical liquid droplets. It is assumed that the liquid is monodispersed; that is, that all droplets are of the same size at one point in the flow and the interactions between droplets are neglected. To make the simulation available and efficient, the condensing steam flow is assumed to be adiabatic and inviscid. Since droplet size are sufficiently small, it is assumed that the volume of the condensed liquid droplets is negligible and the velocity slip between the droplets and gaseous-phase is zero. We have adopted the Eulerian–Eulerian approach for modeling the condensing steam flow. And the two-phase flow is modeled using the conservation-type two-dimensional compressible Navier-Stokes equations, with the transport equations for the liquid-phase mass-fraction (β) and the number of liquid droplets per unit volume (η). Under the foregoing assumptions, the Euler Equations may be written in integral form as follows[16]:

$$\frac{\partial U}{\partial x}+\frac{\partial F}{\partial x}+\frac{\partial G}{\partial x}=0 \qquad (1)$$

Where: x, y and t are the space and time coordinates respectively. U, F and G are defined as:

$$U = \begin{bmatrix} \rho \\ \rho u \\ \rho v \\ \rho E \end{bmatrix}, \quad F = \begin{bmatrix} \rho u \\ \rho u^2 + P \\ \rho uv \\ (\rho E + P)u \end{bmatrix}, \quad G = \begin{bmatrix} \rho v \\ \rho uv \\ \rho v^2 + P \\ (\rho E + P)v \end{bmatrix}$$

And the mixture density, the internal energy and specific enthalpy are determined as follows:

$$\rho = \frac{\rho_g}{1-\beta} \tag{2}$$

$$E = h_0 + \frac{P}{\rho} \tag{3}$$

$$h_0 = h + (u^2 + v^2)/2 \tag{4}$$

$$h = (1-\beta)h_g + h_l \tag{5}$$

To model wet steam, two additional transport equations are needed [4]. The first transport equation governs the mass fraction of the condensed liquid phase (β) and the other transport equation (η) determines the number of droplets per unit volume. The two equations are combined to the model in the following expression:

$$\frac{\partial \rho\beta}{\partial t} + \nabla \cdot (\rho \vec{v}\, \beta) = \Gamma \tag{6}$$

$$\frac{\partial \rho\eta}{\partial t} + \nabla \cdot (\rho\, \vec{v}\, \eta) = \rho I \tag{7}$$

And the number of droplets per unit volume (η) is calculated as

Follows:

$$\eta = \frac{\beta}{(1-\beta)V_d(\frac{\rho_l}{\rho_v})} \tag{8}$$

$$V_d = \frac{4}{3}\pi r_d^3 \tag{9}$$

where ρ_l,V_d, $r_d$denote the liquid density, the average droplet volume and the average droplet radius.

3.2. Nucleation model and droplet growth model for nucleating particles:

The most widely adopted classical nucleation theory is discussed by many authors. In the present study, the non-equilibrium flow calculation considers only homogenous nucleation in pure substance and relies on the classical nucleation theory corrected for non-isothermal effects by **Bakhtar et. Al(2005) [5].**

In the model, the classical homogeneous nucleation theory describes the formation of a liquid-phase in the form of droplets from a supersaturated phase in the absence of impurities or foreign particles, and the nucleation rate is given by:

$$I = \frac{q_c}{1+\theta}\frac{\rho_v^2}{\rho_l}\left(\frac{2\pi RT}{\pi M_m^3}\right)^{\frac{1}{2}} \quad \exp\left(-\frac{4\pi r^{*2}\sigma}{3k_b T}\right) \tag{11}$$

where q_c is the condensation coefficient, K_b is the Boltzmann constant,

M_m is the mass of one molecule, σ is the liquid surface tension, and θ is

a non-isothermal correction factor which is given by the following

relation:

$$\theta = \left[\frac{2(\gamma-1)}{\gamma+1}\frac{h_{lg}}{RT}\left(\frac{h_{lg}}{RT} - 0.5\right)\right] \tag{12}$$

where h_{lv} is the latent heat of evaporation at pressure P. Based on the nucleation model just described the quantity of droplets at a location in the continuous gas phase is known, and the rate at which these droplets grow can be derived on the basis of heat transfer conditions surrounding the droplet [8]. This energy transfer relation can be written as:

$$\frac{d\bar{r}}{dt} = \frac{PCp}{\rho_l h_{lv}\sqrt{2\pi RT}}\frac{(\gamma+1)}{2\gamma}(T_l - T) \tag{13}$$

The mass generation rate Γ in the classical nucleation theory during the non-equilibrium condensation process is given by the sum of mass increase due to nucleation (the formation of critically sized droplets) and also due to growth/demise of these droplets.
Therefore, Γ is written as:

$$\Gamma = \frac{4}{3}\pi\rho_l I r_*^3 + 4\pi\rho_l\eta\bar{r}^2\frac{\partial\bar{r}}{\partial t} \tag{14}$$

Where r* is the Kelvin-Helmholtz critical droplet radius. The droplet will grow as its radius is larger than r* ,otherwise the droplet will evaporate. And r* is given as follows [9]:

$$r^* = \frac{2\sigma}{\rho_l R T \ln S} \tag{15}$$

where S is the super saturation ratio defined as the ratio of vapor pressure to the equilibrium saturation pressure:

$$S = \frac{P}{P_{sat.}(T)} \tag{16}$$

Mach number was calculated from the following equation for isentropic flow **Saad [10]:**

$$M = \sqrt{\frac{2}{\gamma-1}\left[\left(\frac{P_\circ}{P_s}\right)^{\frac{\gamma-1}{\gamma}} - 1\right]} \quad (17)$$

Where P_0 is the stagnation pressure, P_s is the static pressure, γ is the steam specific heat ratio and g=9.81 m/s^2 .

3.3. Equation of state:

The steam equation of state used in the solver, which relates the pressure to the vapor density and the temperature, is given by [29]:

$$P = \rho_g RT\ (1 + B\rho_g + C\ \rho_g^2) \quad (18)$$

Where B,C and are the second and the third virial coefficients given by the following empirical function.

4. RESULTS AND DISCUSSION :

The speed of sound in a two phase mixture is not explicit, and it values depends on the local conditions, while the pressure can be directly measured. For this reason in two phase flows it is prefer able to work in terms of static pressure ratio (P_s/P_0), therefore the isentropic Mach number can be based on this ratio.

Experimentally and numerically the conditions at inlet to the test section could be varied by using throttling valve while back pressure is constant. Static pressure ratio and Mach number distributions for the nozzle against non-dimensional distance along the nozzle are shown in Figs. 7, 8, and 9 for both experimental and numerical. Figs. 7, 8, and 9 show good agreement between numerical and measured distributions for both static pressure ratio and isentropic Mach number.

The shadowgraph photos are used to compare the flow structure and divergent part shock wave with the theoretical velocity vector and droplets growth rate contour as shown in Figs. 10, 11, and 12. It can be seen that the droplet growth rate reach to maximum downstream the throat area of the nozzle due to occurring of condensation process because high expansion rate and decreasing when inlet pressure decrease and its values are (1020,666 and 535) micron/sec. The condensation zone, the area of the propagation of dark region area inside the dotted line envelope, occurred downstream the throat area due to the reduction of inlet pressure. As a matter of fact the dominant effect of phase change in high speed condensing flows is the local departures from thermodynamic equilibrium associate with the sudden release of heat from the droplets. The internal heat transfer associated with phase change is thermodynamically an irreversible process. It is well known that the release of the latent heat by the homogenously nucleating steam flow can have a strong effect on the flow dynamics when the flow is transonic or supersonic with shock waves present. Very interesting results were observed from figs (11 and 12), there is a zone of over expansion on the divergent part and the flow accelerated toward the throat area and then causes to appearance of shock wave and its locations are (123 and 112) millimeters from nozzle entrance.

we can noted that when the static pressure is increased in the shock wave region, an adverse pressure gradient can cause the flow to detach from the nozzle wall surface. This increase in static pressure, which contributes to increased potential energy of the flow, thereby decreases the kinetic energy of the flow. The inner layer of the boundary which is relatively slow is significantly affected by this increasing in static pressure is large enough to bring the velocity to zero or become reversed. This is clear in shadowgraph photos.

5. CONCLUSION:

In general the comparison between experimental and numerical results for the convergent-divergent nozzle flows was found to be fairly acceptable.

1.When the inlet pressure decreases and the outlet conditions is supersonic, the heat release due to condensation process causes a pressure rise in the zone of rapid condensation , which shows up in the shadowgraph photos as a dark zone.

2.When the inlet pressure decreases and the outlet is subsonic, the zone of over expansion appears as a shock wave in the divergent section. The location of this shock wave progress towards the throat when the inlet pressure decreased. This is clear in the shadowgraph photos.

3. The droplet growth rate increased when the inlet pressure decrease.

4. The location of rapid condensation zone has occurred downstream of the throat.

REFERENCES:

[1] A. G. Gerber, "Two-Phase Eulerian/Lagrangian Model for Nucleating Steam Flow". Transactions of the ASME Journal of Fluids Engineering, Vol .124, PP. 465-475, June (2002).

[2] A.J. White, "Numerical investigation of condensing steam flow in boundary layers". International Journal of Heat and Fluid Flow, Vol.21, PP. 727-734, (2000).

[3] A. J. White and J. B. Young, "Time-Marching Method for the Prediction of Two-Dimensional, Unsteady Flow of Condensing Steam". Journal of Propulsion and Power, Vol. 9, No. 4, P.579, July-Aug. (1993).

[4] ANSYS FLUENT 15.0 Theory guide.

[5] F. Bakhtar, J.B. Young, A.J. White and D.A. Simpson,"Classical nucleation theory and its application to condensing steam flow calculations". Proc. IMech. Vol.219, part c: J. Mechanical Engineering Science ,(2005).

[6] G. Cinar and B. S.Yilbas, "Experimental Study into Droplet Formation in Steam Flows". Kluwer Academic Publishers,(1998).

[7] Guha and J. B. Young, "Time-marching prediction of unsteady condensation phenomena due to supercritical heat addition". IMechE, pp.167-177, (1991).

[8] H.W. Mashi and S. A. Alrabii," Drop Diameter Prediction Model for Liquid Phase Dispersion In A Supersonic Nozzle with Wet Steam Flow". Journal of Engineering and Development, Vol. 16, No.4, Dec. (2012).

[9] J. Halama, J. Fort, "Homogeneous Nucleation of Steam In Convergent-Divergent Nozzle". Engineering Mechanics, Vol. 21, No.3, p. 145–150, (2014).

[10] M. A. Saad,"Compressible fluid flow". Prentaice-Hall, Inc. Englewood Cliffs, New Jersey,1985.

[11] M.H. Kayhani, S. Zarenezhad, E. Lakzian and S.M. Hashemia, " Numerical Investigation of 2D Condensation Steam Flow by Eulerian-Eulerian Method". International Conference on Mechanical, Automobile and Robotics Engineering, Malaysia,(2012).

[12] M.J. Kermani and A.G. Gerber," A general formula for the evaluation of thermodynamic and aerodynamic losses in nucleating steam flow". international journal of jet and mass transfer, Vol. 46, pp. 3265-3278, (2003).

[13] M. J. Kermani, A. G. Gerber and J. M. Stockie, "Thermodynamically Based Moisture Prediction Using Roe's Scheme". 4th Conference of Iranian Aero Space Society, (2003).

[14] M. McCallum and R. Hunt, "Numerical solution of the flow of wet steam in a steam turbine using an Eulerian code". 17th Dudee Numerical Analysis Conference, June 24-27, (1997).

[15] S. Senoo and Y. Shikanow,"Two-Dimensional Analysis for Non-Equilibrium Homogeneously Condensing Flows through Steam Turbine Cascade". JSME International Journal, Series B, Vol.45, No.4, (2002).

[16] Yong Yang and Shengqiang Shen, "Numerical simulation on non-equilibrium spontaneous condensation in supersonic steam flow". International Communications in Heat and Mass Transfer 36 (2009) 902–907.

Table (1): Dimensions of the selected nozzle.[8]

Width(B) (mm)	*Height (H) (mm)*	*Length(L) (mm)*	$\frac{L_1}{L}$	$\frac{L_2}{L_1}$	$\frac{A_1}{A_2}$
60	**100**	**140**	**0.628**	**0.59**	**0.71**

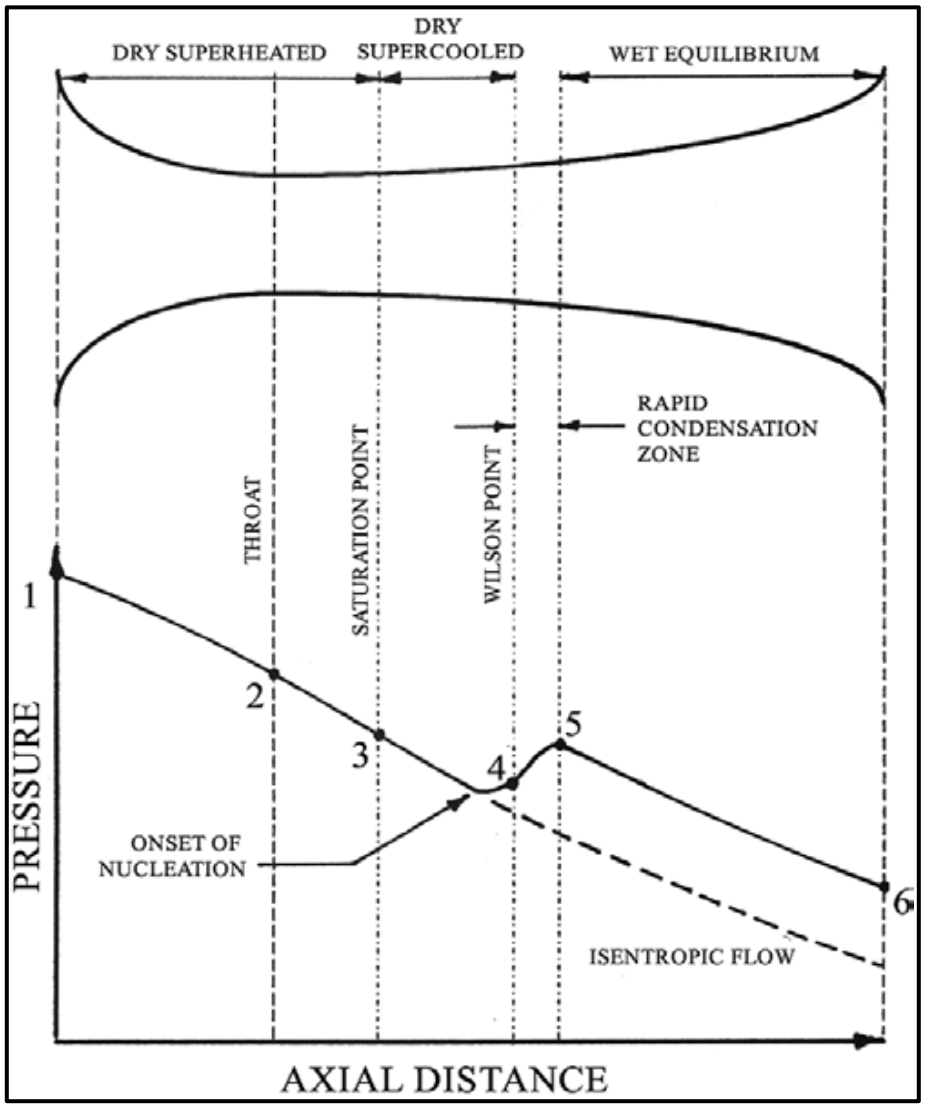

Figure (1): Pressure distribution along a convergent-divergent nozzle with spontaneous condensation.[11]

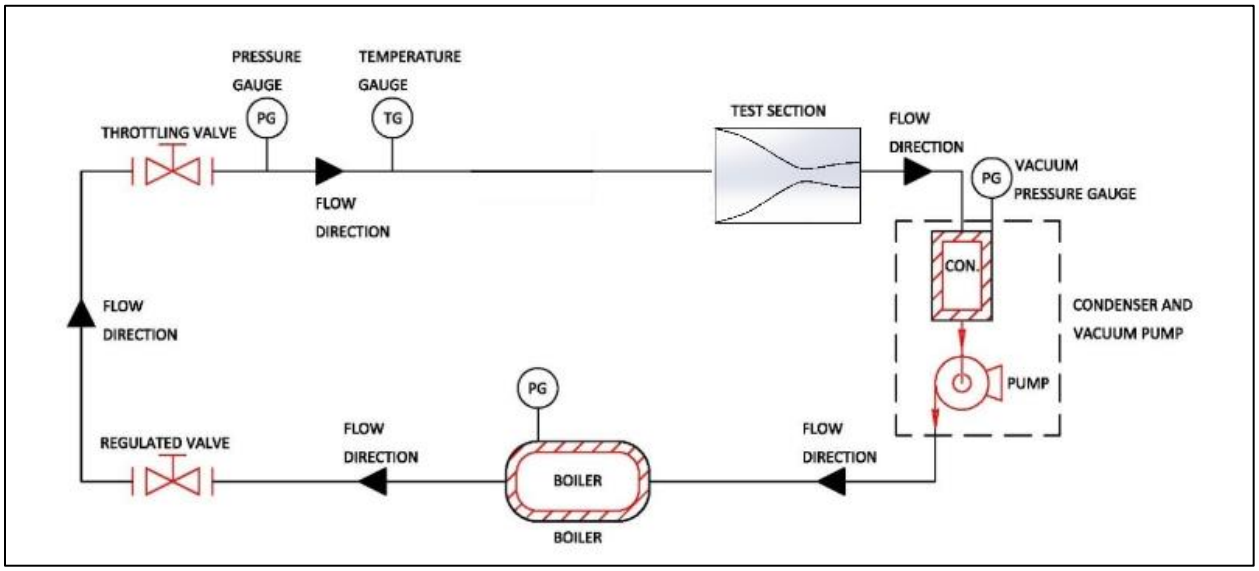

Figure (2): The system schematics diagram

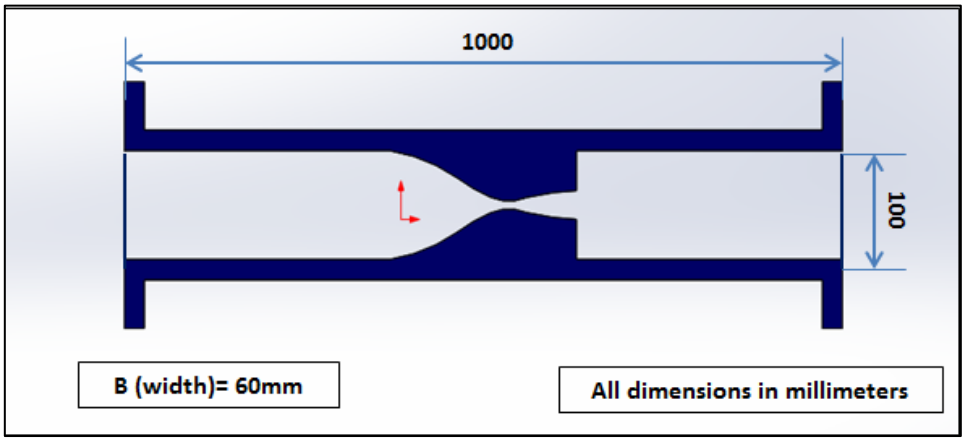

Figure (3): The tunnel dimensions from research conducted in Moscow P.E.I.[8]

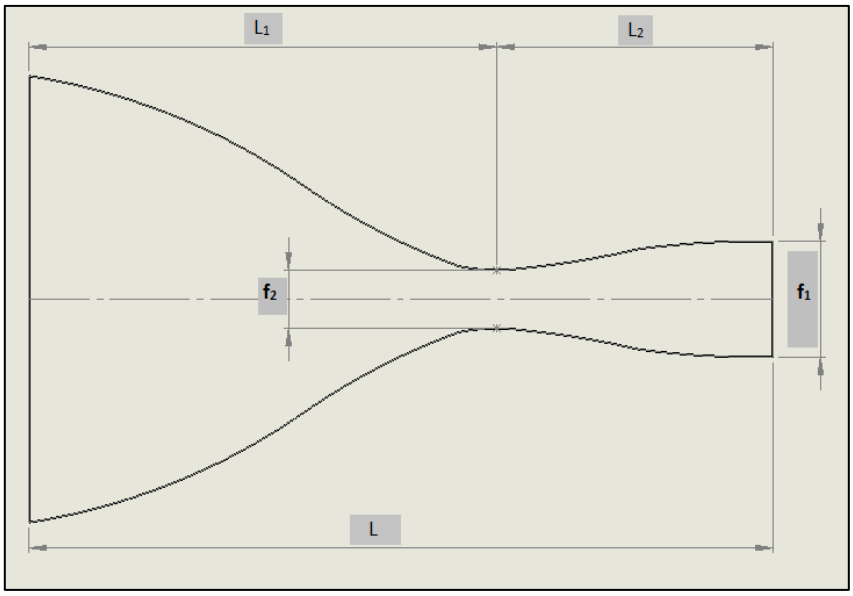

Figure (4): C-D Nozzle schematics diagram from research conducted in Moscow P.E.I.[8] .

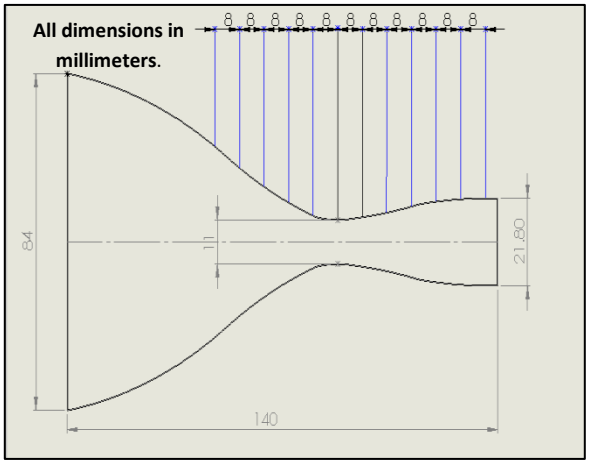

Figure(5): Spacing between pressure taps of modified nozzle.

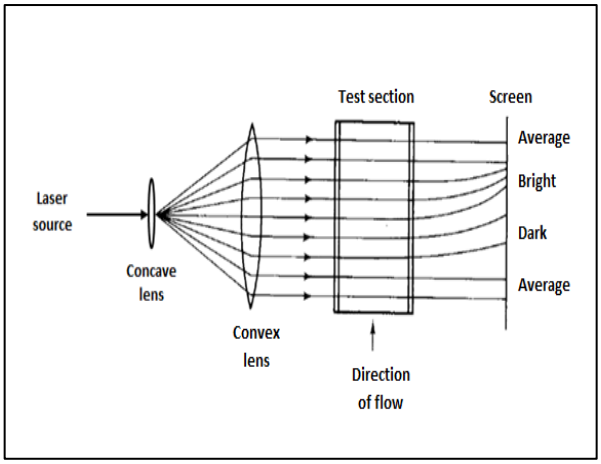

Figure(6): Shadowgraph schematics diagram

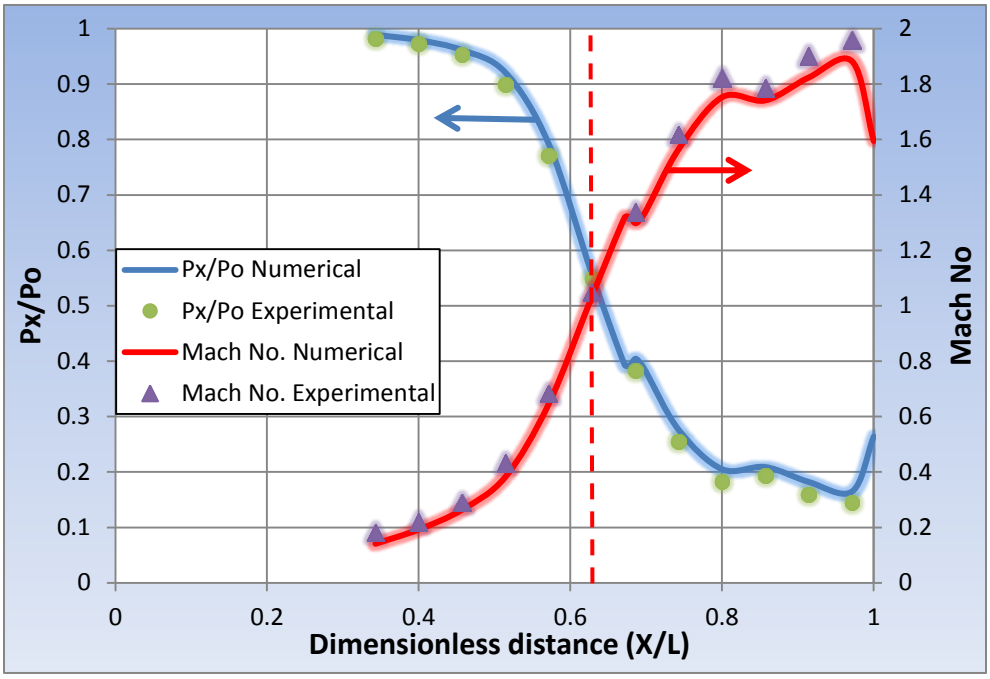

Figure (7): The experimental and numerical pressure ratio and Mach No. distribution at (P_0 =0.69 bar , T_0=362 K , ε_0=0.29 and P_b=0.2 bar)

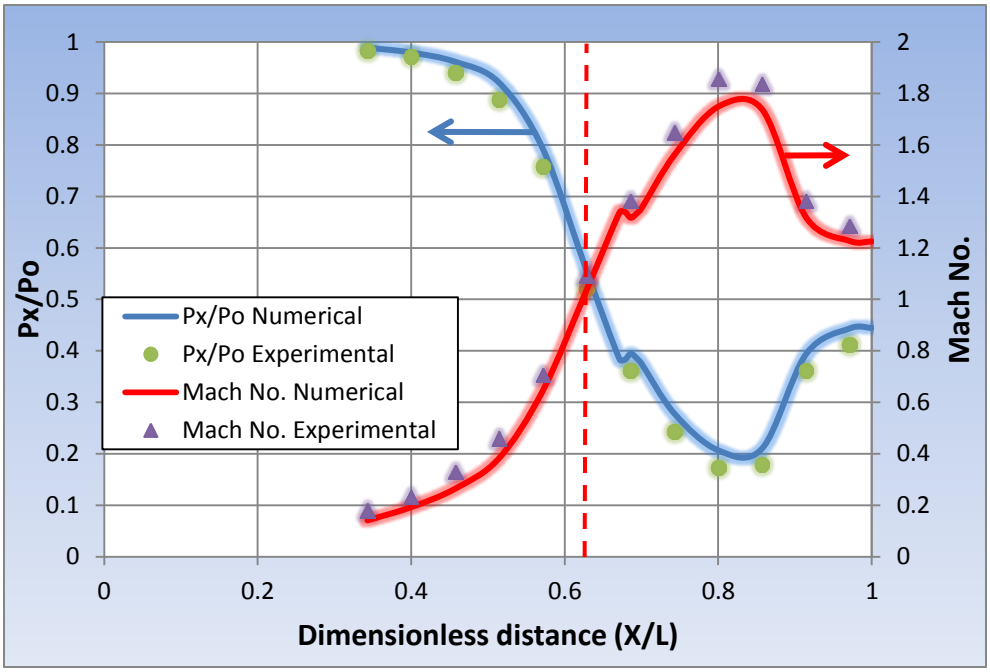

Figure (8): The experimental and numerical pressure ratio and Mach No. distribution at

(P_0 =0.45 bar , T_0=352 K , ε_0=0.44 and P_b=0.2 bar)

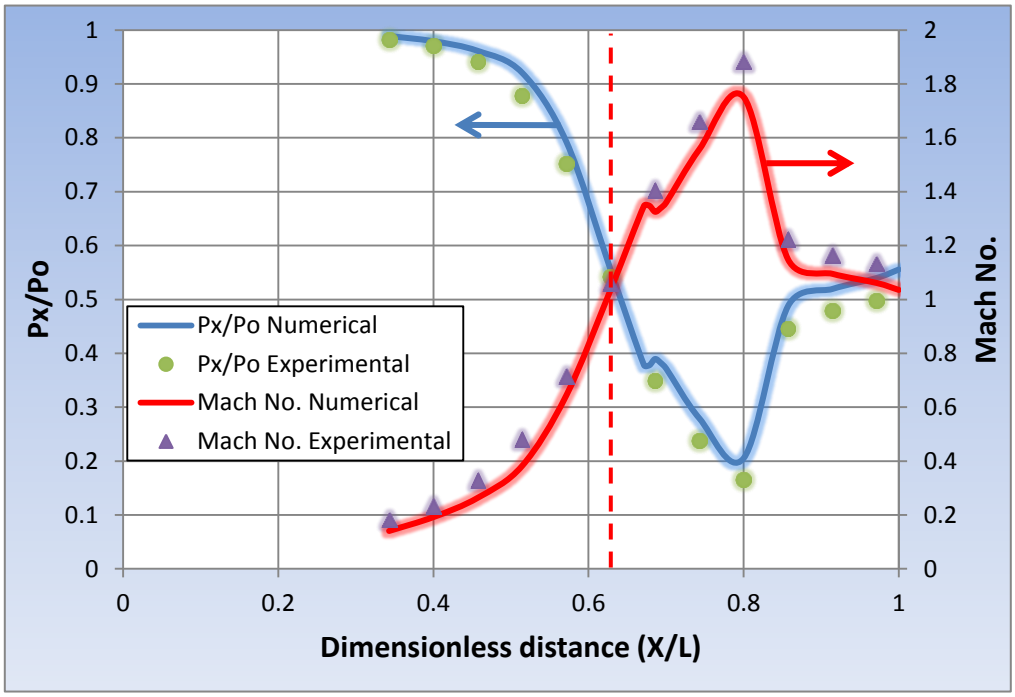

Figure (9): The experimental and numerical pressure ratio and Mach No. distribution at (P_0 =0.36 bar , T_0=346 K , ε_0=0.55 and P_b=0.2 bar)

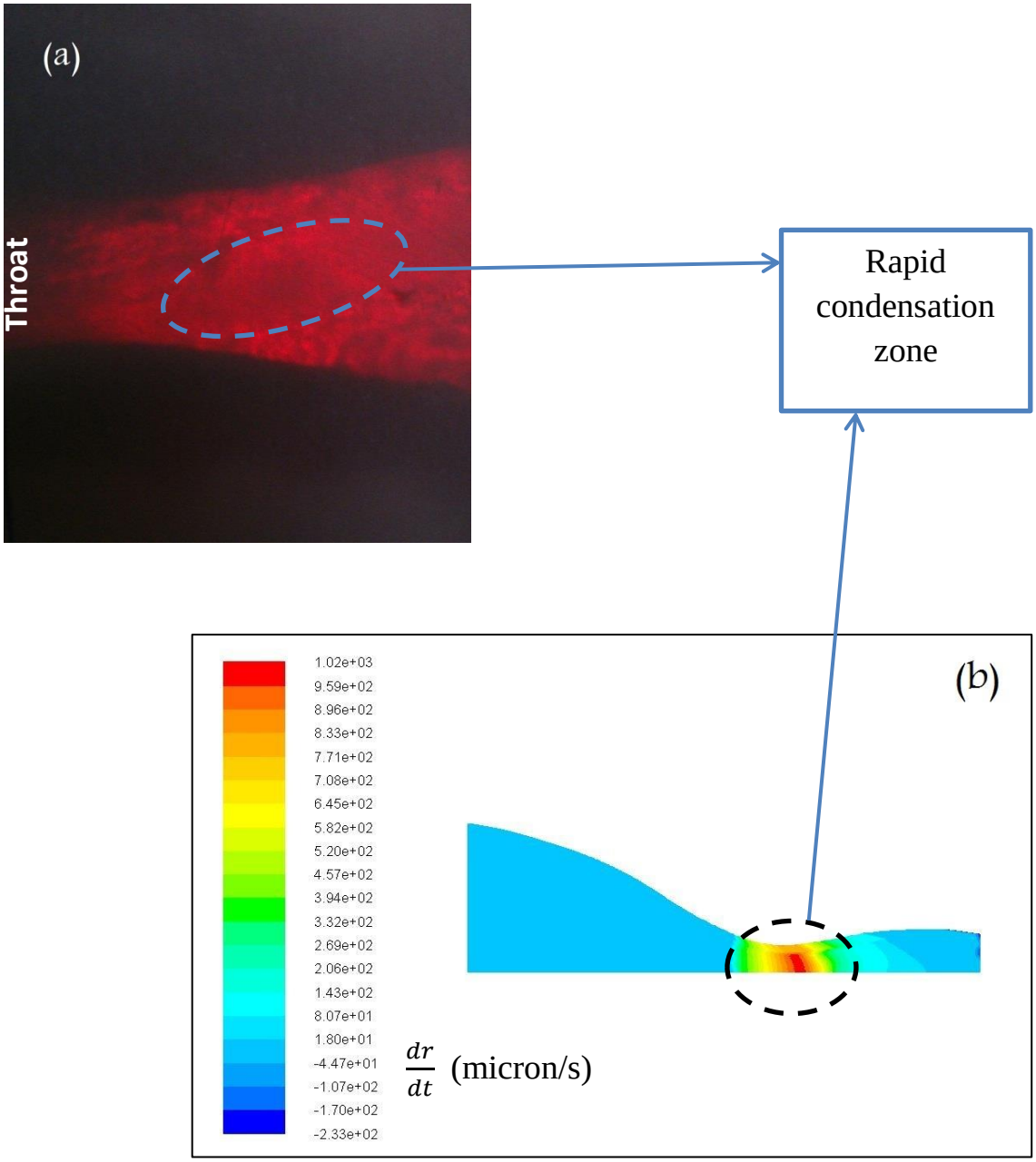

Figure (10): (P_o =0.69 bar , T_o=362 K ,P_b=0.2 bar). (a) shadowgraph photo.

(b) The predicted droplet growth rate contour

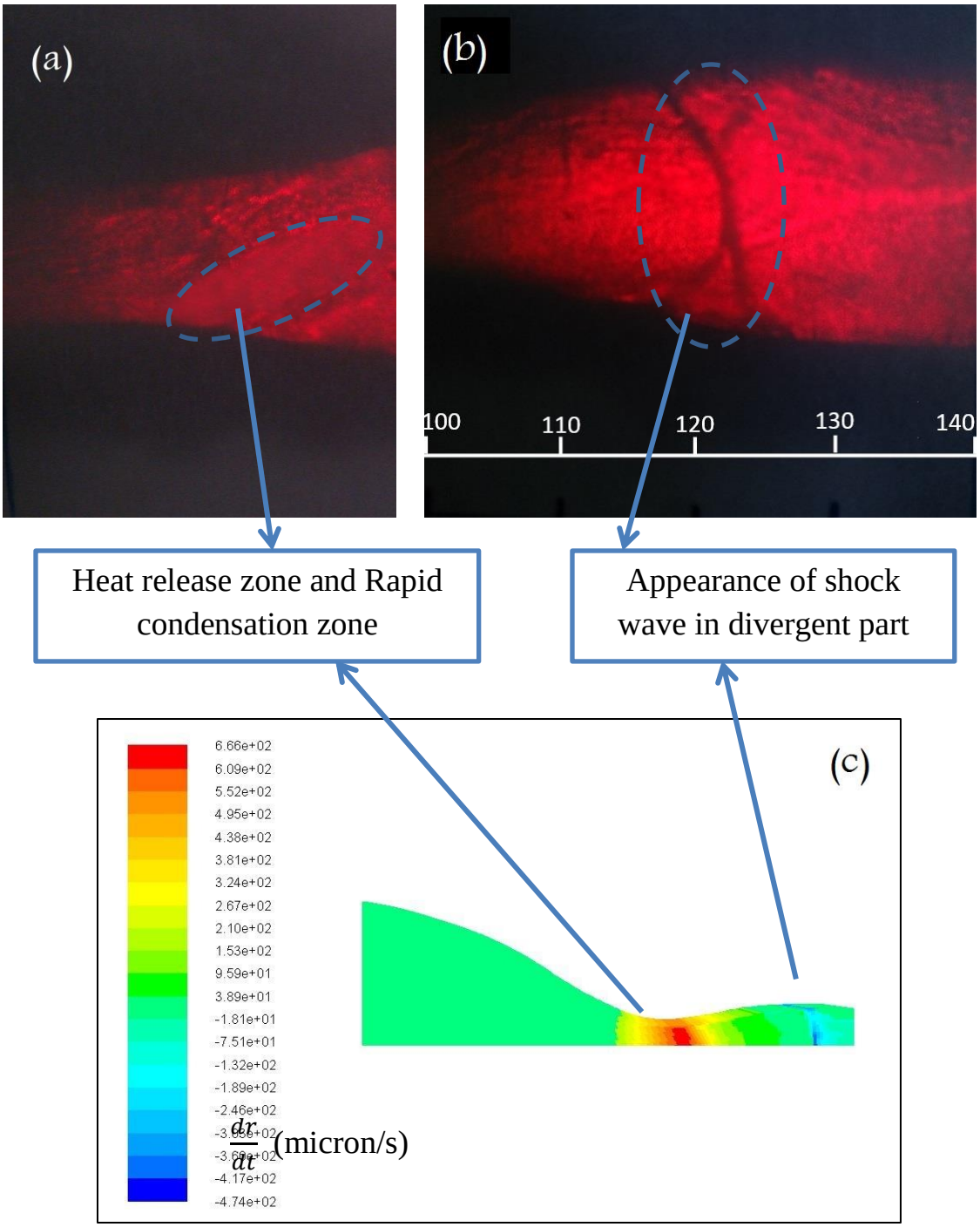

Figure (11): (P_o =0.45 bar , T_o=352 K ,P_b=0.2 bar). (a) and (b) shadowgraph photos for the throat and divergent part respectively. (c) The predicted droplet growth rate contour

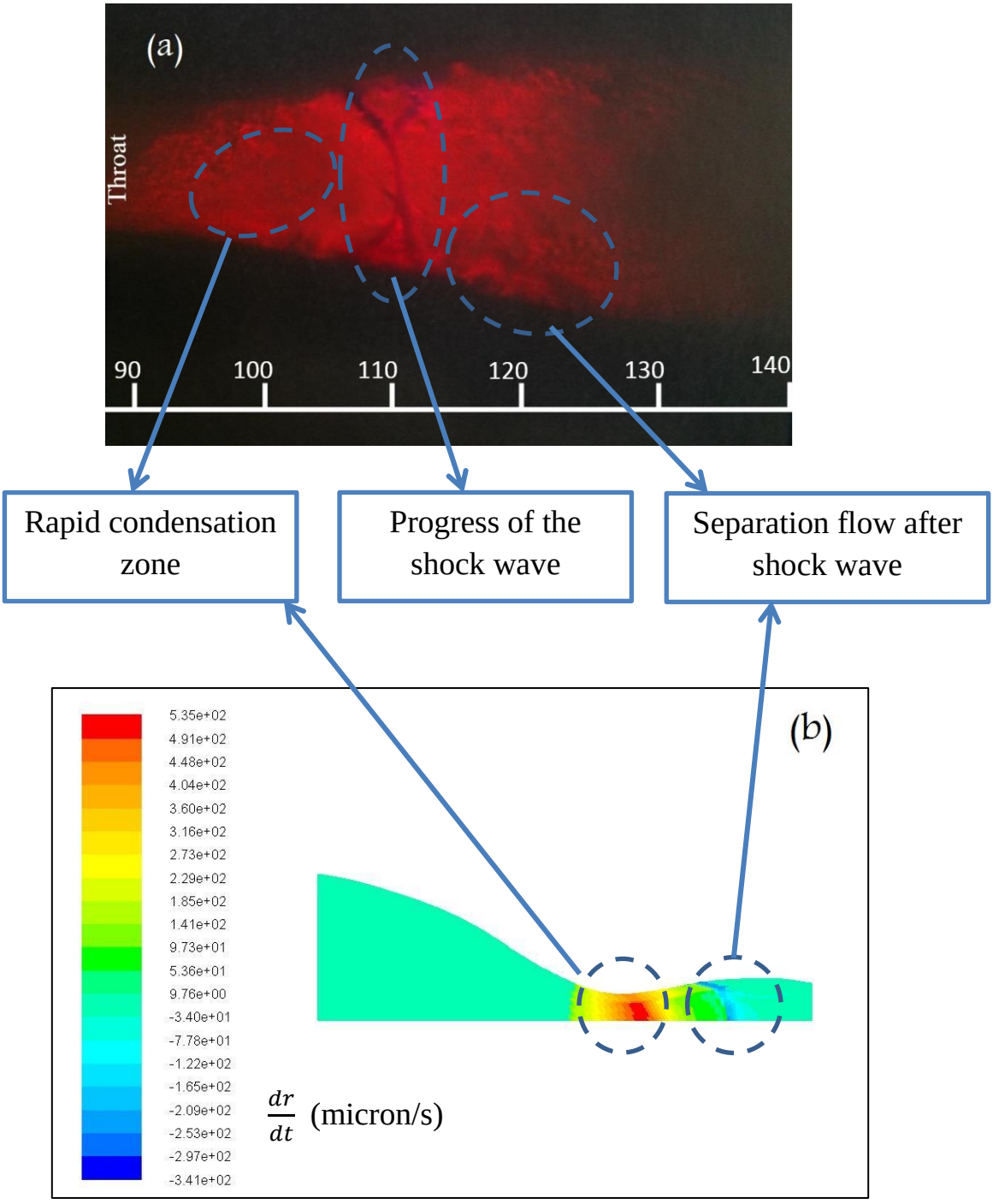

Figure (12): (P_o =0.36 bar , T_o=346 K ,P_b=0.2 bar). (a) shadowgraph photo.

(b) The predicted droplet growth rate contour